Hindawi
Shock and Vibration
Volume 2019, Article ID 2076961, 13 pages
https://doi.org/10.1155/2019/2076961

Research Article

Seismic Acceleration Spectrum of Ground Surface under Urban Subway Tunnels with Circular Cross Sections in Soil Deposits Based on SSI

Hamed Fakhriyeh, Reza Vahdani, and Mohsen Gerami

Department of Seismic Engineering, Faculty of Civil Engineering, Semnan University, Semnan, Iran

Correspondence should be addressed to Reza Vahdani; rvahdani@semnan.ac.ir

Received 8 May 2019; Revised 29 July 2019; Accepted 3 October 2019; Published 5 December 2019

Academic Editor: Hassan Haddadpour

Underground tunnels with circular cross section nowadays have great application in the field of transportation. One of their most prominent uses is the subway, built with the help of tunnel boring machines (TBMs). The design of ground-surface structures in the far field is related to the horizontal component of the peak ground of acceleration. Therefore, in this study, we tried to change the frequency of the soil-tunnel system by changing the overburden depth, diameter, and lining thickness of the tunnel, as well as changes in the soil specification, and calculate the maximum acceleration of the ground's surface in the presence of the tunnel. The relationship between the peak horizontal acceleration of the ground surface and the frequency of the soil-tunnel system will result in the production of a horizontal acceleration spectrum. The results show that the amplification of ground surface depends on the period of the soil-tunnel system, the characteristics of the model, and the status of the point studied at the ground surface relative to the tunnel. On the projection of the center of the tunnel on the surface of the ground, the presence of the tunnel, rarely, at a long period, is effective in amplifying the spectral acceleration. While moving away from the image of the center of the tunnel on the surface of the ground, the presence of the tunnel in many cases, in long periods, amplifies spectral acceleration. The presence of the tunnel amplifies the spectral acceleration on the ground surface above 11%, while the presence of a tunnel reduces the spectral acceleration on the ground surface by up to 15% (attenuation). Using Plaxis 2D and Ansys finite element software, the case study was conducted on a Delhi subway tunnel with horizontal components of acceleration records similar to the construction site.

1. Introduction

The rapid growth of urban populations and the lack of space on the ground have led to an increase in underground structures. One of the most widely used underground structures is subway tunnels, which are excavated with TBM. The effectiveness of this type of structure under earthquake has been considered by numerous researchers in numerical and experimental methods [1–4]. In underground subway tunnels, the interaction of soil and structure, especially for tunnels that are excavated in soil deposits, is considered. The effect of underground structures on the ground surface's seismic responses has been studied by researchers, and it has been concluded that the presence of underground structures is effective in seismic responses of the ground's surface [5–8].

Maximum ground surface acceleration is one of the important parameters in the design of ground structures, especially in the far field, which can be subjected to underground structures. However, the effect of these underground structures has not been included in the codes for the ground surface structural design. Different analytical solutions examine the effects of underground cavities on ground-generated motion by using P, S, and Rayleigh seismic waves [9–14]. But in these methods, simplified assumptions such as the elasticity of the medium are used and the effects of nonlinearity of the soil are not considered. Yiouta-Mitra et al. [5] studied the effect of soil medium characteristics, tunnel diameter, overburden depth, relative flexibility of the lining of the tunnel, and frequency of excitation on ground surface acceleration. The results indicate

the impact of underground structures on the acceleration of ground surface. Sun and Wang [15] examined the difference in ground surface acceleration in free-field conditions and the presence of underground structures. The results show the high impact of underground structures on PGA and response spectrum. Baziar et al. [6] examined the effect of rectangular tunnels on the acceleration of the ground's surface by using the centrifugation model and numerical solutions. It was concluded that the presence of the tunnel causes an attenuation of acceleration in short periods and amplifies ground surface's acceleration for long periods. Raghavendra et al. [16] analyzed the underground metro tunnels. Their study high lights the elastic and elastoplastic analysis of the twin tunnel system subjected to gravity and hydrostatic pressure conditions combined with blast-induced pressures.

Marshall and Haji [17] studied the relationship tunnel-pile interaction. Their study illustrated the importance of considering the specific geometry of each case due to the sensitivity of results to the depth of the pile and tunnel. Sevim [18] studied 3D earthquake response of the Arhavi Highway Tunnel considering soil-structure interaction. This study describes earthquake response of the Arhavi Highway Tunnel and its geometrical properties, the 3D finite element model, and the linear time-history analyses under a huge ground motion considering soil-structure interaction. The results obtained from the 3D finite element model are presented. In addition, the displacement and stress results are observed to be the allowable level of the concrete material during the earthquakes. Zheng et al. [19] studied the traditional Lagrangian finite element and Eulerian finite element methods for stability analysis of circular tunnels in undrained clay.

In most of the studies cited above, monolayer soils were used, but there are urban subway tunnels excavated in multilayer soil. For example, we can mention the tunnel of the Delhi subway. In this study, the effect of the presence of a circular tunnel on the ground surface acceleration was investigated. Eleven acceleration records from known major earthquakes, 36 models incorporating the presence of a tunnel, and seven models without a tunnel were used. A total of about 500 nonlinear dynamic analyses were performed. The analyses were carried out for multilayer soil with regard to the nonlinear effects of soil and the interaction of soil and structure.

Generally, during the design process, two levels of ground motion are commonly considered: service-level ground motion and the maximum considered earthquake (MCE). However, response-spectrum analysis is sufficient to evaluate a structure for the service-level motion during which the structure is expected to remain elastic, and dynamic time-history analysis is usually recommended or required to capture the nonlinear behavior of a structure subjected to MCE motion [20]. The standard shape of the response spectrum was the uniform hazard response spectrum in IBC [21] and NEHRP [22] provisions. Predictive models that provide the spectral ordinates of ground motion required for response-spectrum analysis include the recently developed and commonly used NGA ground motion prediction equations by [23–27].

2. Numerical Modeling

Two-dimensional plane strain dynamic finite element (FE) analysis was performed for a subway tunnel with a rectangular domain. The dimensions of the model in PLAXIS 2D [28] were 60×140 m. Fifteen nodal triangular elements were considered for the soil mass, and the tunnel lining with a plate element was linearly modeled. In Ansys [29], modal analysis using similar dimensions was carried out in Plaxis 2D. The Drucker–Prager model was used for nonlinear soil properties and frequency-independent damping. Regarding the previous studies which have been conducted, the behavioral model used for soil in Plaxis is Moher–Coulomb [6–8, 30–32].

2.1. Soil Properties. The Delhi subway has been excavated in soil deposits. Modifications to the soil elasticity modulus with depth are summarized in Table 1. Unit weight and saturated unit weight of soil are 18 and 20 kN/m^3, respectively. No water table is present, and the cohesion (c) of the soil is zero. The friction angle (φ) and angle of dilation (ψ) are 35° and 5°, respectively. Poisson's ratio of the soil was 0.25. To consider the interaction between the tunnel and its surrounding soil, R_{inter} was used in Plaxis 2D. This parameter is related to the soil strength to the interface strength which is represented by the following equation:

$$\begin{aligned} \tan(\varphi)_{\text{interface}} &= R_{\text{inter}} \cdot \tan(\varphi)_{\text{soil}}, \\ C_{\text{inter}} &= R_{\text{inter}} \cdot C_{\text{soil}}. \end{aligned} \tag{1}$$

Hence, using the entered R_{inter}-value gives a reduced interface friction angle and interface cohesion compared to the friction angle and the cohesion in the adjacent soil. In other words, the R_{inter} size must be less than one. According to the soil properties, the value of R_{inter} in this study was 0.67.

2.2. Tunnel Properties. Similar to previous studies, the behavior of the tunnel lining was considered to be elastic. The diameter of the tunnel in the original model (Delhi subway) is 6.26 meters, and the overburden depth is 16.87 meters. The thickness of the tunnel lining is 0.28 m, and the reinforced concrete with the modulus of elasticity (E_c) is equal to 3.16×10^7 kPa and the Poisson ratio (υ) is equal to 0.15.

2.3. Damping. A common parameter used in damping is the damping ratio (ξ). In the FE method, Rayleigh's damping is one of the appropriate measurements which bears the damping effects in the stiffness matrix and system mass. In plain strain models such as tunnels in two-dimensional models and applying earthquake, Rayleigh damping seems necessary to obtain results that are consistent with reality, and the general form is given as follows:

$$[C] = \alpha[M] + \beta[k], \tag{2}$$

where M and K are the mass and stiffness matrices, respectively, and α and β are the Rayleigh damping coefficients. Rayleigh alpha is a parameter that determines the mass effect on the system's damping. Rayleigh beta is a

Table 1: Modulus of elasticity versus depth for Dehli subway soil [32].

Depth (m)	Thickness (m)	Modulus of elasticity (kpa)
0–10	10	7500
10–20	10	15000
20–35	15	30000
35–50	15	40000
50–60	10	50000

parameter that determines the effect of stiffness on the system damping. These coefficients are determined by the following equation:

$$\alpha = \frac{2\omega_n \cdot \omega_m \left(\xi_n \cdot \omega_m - \xi_m \cdot \omega_n\right)}{\omega_m^2 - \omega_n^2},$$
$$\beta = \frac{2\left(\xi_m \cdot \omega_m - \xi_n \cdot \omega_n\right)}{\omega_m^2 - \omega_n^2}. \quad (3)$$

In equation (3), ξ is the damping ratio and ω_n and ω_m are the natural frequencies of the set in rad/sec, respectively, for the modes shape of n and m. In the present study, m and n were considered as 1 and 2, respectively. Using the Ansys software, the modes shape and frequency of the soil-tunnel system were calculated. Assuming a damping of 5%, Rayleigh's α and β coefficients were obtained and used in Plaxis.

2.4. Models under Study. To create the frequency and mode shapes for the study, various models for soil and tunnel specification were considered. For the soil, models including the actual model of the Delhi subway and 1.25 and 1.5 times the modulus of elasticity, also 1.75 and 2 times the elasticity modulus, and finally 2.25 and 2.5 times the modulus of elasticity of the main soil model of the Delhi subway were used. Also, the tunnel with diameters, lining thicknesses, and different overburden depths is considered, which are summarized in Table 2.

2.5. Earthquake Loading. Eleven different acceleration records have been applied to the models. The acceleration records were selected from the PEER [33] website. The acceleration record characteristics are summarized in Table 3. PGA of all acceleration records has been scaled to 0.35 g (PGA for very high-risk areas under the regulation of 2800 Iran [34] is 0.35 g). This process is done with SeismoSignal software. Considering that the soil excavated in the Delhi subway tunnel is a soil deposit with a shear wave velocity of less than 175 m/sec, therefore, the selected acceleration records, as shown in Table 3, are in the soil with a shear wave velocity (Vs) of less than 175 m/s. Also, the predominant period of acceleration records was calculated with SeismoSignal software, and along with the PGV value and the duration of earthquakes and their PGA, they are presented in Table 4 before being scaled up. The mentioned parameters are effective in the shape and amount of the acceleration spectrum.

Table 2: The models studied in the present research.

No.	Elasticity module of soil (compared to Delhi Metro)	Overburden depth (m)	Lining thickness (m)	Tunnel radius (m)
1	1	20	0.5	3.13
2	1	20	0.28	3.13
3	1	10	0.5	6
4	1	10	0.75	6
5	1	20	0.75	6
6	1.25	10	0.28	3.13
7	1.25	20	0.28	3.13
8	1.25	10	0.5	6
9	1.25	20	0.5	6
10	1.5	20	0.5	3.13
11	1.5	20	0.28	3.13
12	1.5	10	0.75	6
13	1.5	10	0.5	6
14	1.5	20	0.5	6
15	1.5	20	0.75	6
16	1.75	10	0.28	3.13
17	1.75	20	0.28	3.13
18	1.75	10	0.5	6
19	1.75	20	0.5	6
20	2	20	0.5	3.13
21	2	20	0.28	3.13
22	2	10	0.75	6
23	2	10	0.5	6
24	2	20	0.5	6
25	2	20	0.75	6
26	2.25	10	0.28	3.13
27	2.25	20	0.28	3.13
28	2.25	10	0.5	6
29	2.25	20	0.5	6
30	2.5	20	0.5	3.13
31	2.5	20	0.28	3.13
32	2.5	20	0.5	6
33	2.5	10	0.5	6
34	2.5	10	0.28	3.13
35	1	20	0.5	6
36	1	10	0.28	3.13

2.6. Boundary Conditions. The model has 140 m width and 60 m depth which is created for free-field and tunnel interaction analysis. The distance of the vertical model boundaries from each other was selected so that the refraction and reflection of the seismic waves can be avoided to the model, and the model has free-field conditions. Besharat et al. and Singh et al. [8, 32] considered a tunnel diameter that is five times larger (5D) than each side as an appropriate dimension to reach free-field conditions. For static analysis, the nodes were restrained in the x direction along the vertical boundaries of the FE mesh, but they were free to move in the y direction. In the bottom boundaries, the nodes were restrained in both the x and y directions. Two boundary conditions were examined for dynamic analysis in a numerical model: Which includes the absorbing boundary and the free-field boundary. The former was used for the model base and the latter for the free field for the model sides. The absorbing boundaries which are at the bottom prevented the wave reflection into the model, and the free-field boundaries

Table 3: Properties of acceleration records for time-history analysis.

No.	RSN	Mag	Component name	Event	Year	Rjb (km)	Rrup (km)	Vs30 (m/s)
1	326	6.36	H-C02000	Coalinga-01	1983	43.83	44.72	173.02
2	452	6.19	A01040	Morgan Hill	1984	53.89	53.89	116.35
3	732	6.93	A02043	Loma Prieta	1989	43.06	43.23	133.11
4	1843	5.0	A02090	Yountville	2000	94.18	94.5	133.11
5	3697	5.27	B-WAT180	Whittier Narrows-02	1987	26.14	29.09	160.58
6	3828	5.0	TIGA090	Yountville	2000	60.29	60.79	155.11
7	759	6.93	A01000	Loma Prieta	1989	43.77	43.94	116.35
8	962	6.69	WAT180	Northridge-01	1994	45.44	49.81	160.58
9	608	5.99	A-WAT180	Whittier Narrows-01	1987	26.3	30.03	160.58
10	732	6.93	A02133	Loma Prieta	1989	43.06	43.23	133.11
11	962	6.69	WAT270	Northridge-01	1994	45.44	49.81	160.58

Table 4: Properties of acceleration records were calculated by the SeismoSignal.

No.	PGA (g)	PGV (Cm/s)	Predominant period (sec)	Time (sec)	Duration of the strong ground motion (D5-95) (sec)
1	0.1097	11.598	0.44	59.98	17.8
2	0.04295	3.725	0.3	59.98	35.7
3	0.2744	53.652	1.06	35.96	11.8
4	0.00796	0.7797	0.46	47.995	15.3
5	0.0475	5.007	0.7	22.65	12.3
6	0.00897	0.47518	0.14	59.99	30.6
7	0.2576	31.935	0.5	59.99	23.1
8	0.09145	6.332	0.3	39.98	23.4
9	0.11015	8.88	0.3	29.65	15.1
10	0.2203	34.118	0.66	35.955	11.8
11	0.08826	8.321	0.28	39.98	23.4

were used to create free-field conditions at the lateral boundaries of the model (Figure 1). For dynamic analysis, the viscous adsorbent boundaries which were proposed by [35] were used to change the displacement conditions in both directions for vertical boundaries.

2.7. Meshing. Kuhlemeyer and Lysmer [36] showed that for a precise representation of wave transfer of a model, the element size (ΔL) should be one tenth to one eighth of the wavelength associated with the highest component of the input wave frequency. That is,

$$\Delta l \leq \frac{\lambda}{10} - \frac{\lambda}{8}, \tag{4}$$

where λ is the wavelength for the wave propagated in the model. λ is related to the soil shear wave velocity (V_s) and the highest input wave frequency (f_{Max}) according to the following equation:

$$\lambda = \frac{V_s}{f_{Max}}. \tag{5}$$

By replacing equation (4) with equation (5), the following equation is obtained:

$$\Delta l \leq \frac{V_{s\,min}}{10 \cdot f_{Max}}. \tag{6}$$

Considering the least soil shear wave velocity for all models and also the maximum input wave frequency for eleven earthquake records applied, the element size was considered as one meter. To achieve more precision, the mesh was refined around the tunnel.

2.8. Stages to Analysis. Modal analysis was performed to calculate the mode shape and the vibration frequencies of the soil-tunnel systems. To analyze the nonlinear time history for calculating acceleration, the following three phases were considered:

(i) Plastic analysis and staged construction. In this step, the lining of the tunnel was activated and the soil inside the tunnel was deactivated.

(ii) Stress created on the ground caused the tunnel lining to contract, which deformed the lining and changed its volume. In the second phase, the amount of reduced volume is simulated by applying the contraction to the tunnel lining. This contraction will be defined in the phase of in-stage construction calculation, and the contraction of 2% will be applied to the tunnel center.

(iii) In the third phase, dynamic time-history analysis was carried out and the earthquake record was applied to the model once the plastic analyses were complete.

In Plaxis, for numerical time integral calculations, the implicit Newmark design is used. The appropriate time of the step length proposed by Newmark is one-fifth to

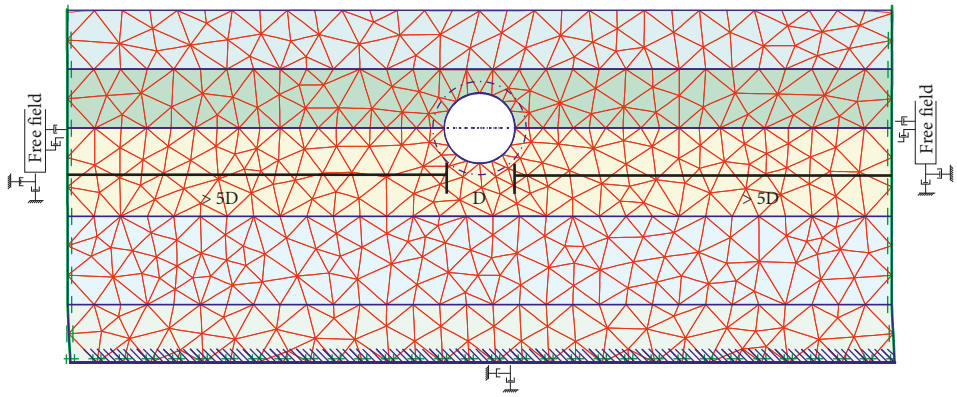

Figure 1: Schematic illustration of boundary conditions and dimensions of the model.

one-sixth of the smallest amount of the system period (Tn). In Plaxis, the time step used in dynamic calculations is constant and equal to $\delta t = \Delta t/m \cdot n$, such that Δt is the time of dynamic loading, n is the number of additional steps, and m is the number of alternative stages. The number of additional steps in this study was 250. In the Newmark method, the optimal parameters selected are $\beta = 0.3025$ and $\gamma = 0.6$, which was used in Plaxis.

2.9. Verification. Sevim's study was used for the verification of modeling and modal analysis. He studied the nonlinear behavior in the Turkish metro named Arhavi based on Erzincan earthquake in 1992 by Ansys. The study by Singh et al. [32] was used for the verification of modeling and time-history analysis. They studied the seismic response in Delhi's subway tunnels by finite element Plaxis software and Rayleigh's damping based on horizontal and vertical components in Uttarkashi's earthquake. Results are shown in Figures 2 and 3. As shown in Figures 2 and 3, the diagrams are close to each other.

3. Review of Modal Analysis Results

Dobry et al. [38] proposed a predominant natural period for soil deposits as $T = 4h/c_s$, where h is the thickness of the alluvial layer and C_s is the shear wave velocity. However, this equation and a similar equation for single-layer soils are accurate and do not have the proper accuracy for multilayer soils (similar to those in the present study). Therefore, using Ansys software, the values of the frequency and the main period of the vibration of the model, as well as the modes shape for all the models mentioned in Table 2 were done. The frequencies and vibration modes of the first and second for model 4 of Table 2 are shown in Figure 4.

Then, using equation (3), the α- and β-Rayleigh values were calculated and used in Plaxis software as one of the input data. From the modal analysis, it was determined that the frequency of the soil-tunnel system is more dependent on the modulus of soil elasticity. The variation in the depth of the tunnel placement and the diameter and thickness of the tunnel lining are very different from those of the soil elastic modulus. Table 5 gives the results of modal analysis, including the frequencies of the first and second modes and Rayleigh α and β for all models in Table 2. The ordering of the numbering of the models in Table 5 is similar to Table 2. By increasing the modulus of soil elasticity in the models, Rayleigh's alpha value is increased and Rayleigh's beta value decreases.

4. Time-History Analysis

In this section, the sensitivity analysis and the acceleration spectrum due to the presence of the tunnel were evaluated as follows.

4.1. Sensitivity Analysis. Sensitivity analysis was performed to identify the influence of each input variable on the output parameters [39]. By analyzing the time history of the software Plaxis 2D, it was determined that the acceleration history of the key points of the model was dependent on the soil mechanical parameters such as friction angle (φ), cohesion (C), dilation angle (ψ), soil unit weight (γ), and Poisson's ratio (υ). Changes in soil unit weight (γ) have no significant effect on maximum acceleration, and by reducing soil unit weight from 18 to 14 kN/m^3, only 1% of the decrease in maximum ground acceleration is observed. By decreasing soil the unit weight from 18 to 16 kN/m^3 (12.5% reduction in soil unit weight), the 7% increase is seen in maximum acceleration. Due to an increase in soil unit weight from 18 to 20 kN/m^3, an increase of about 11% in soil unit weight, about 3.5% increase in maximum acceleration of the ground's surface is observed.

Also, the effect of friction angle (φ) and soil dilation angle (ψ) on the maximum acceleration from the center of the tunnel projection onto the ground surface was investigated. By reducing the friction angle of the soil from 35 to 20 degrees and the dilation angle from 5 degrees to zero, in other words, with a decrease of about 43% at the friction angle of the soil, about 26% decrease in the maximum acceleration of the ground's surface occurs. Also, by reducing the friction angle of the soil from 35 to 30, and the dilation angle, from 5 to zero degrees, in other words, decreasing about 14.5% at the friction angle of the soil, is observed about 13% decrease in the maximum acceleration of the ground's surface. In addition, the effect of increasing the friction angle from 35 to 40 degrees on the maximum acceleration from

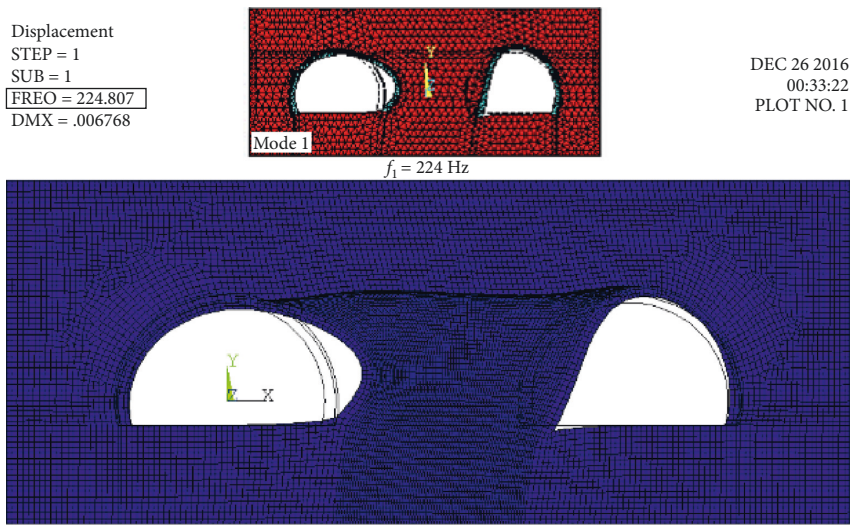

Figure 2: Verification of modal analysis with the study bySevim [37].

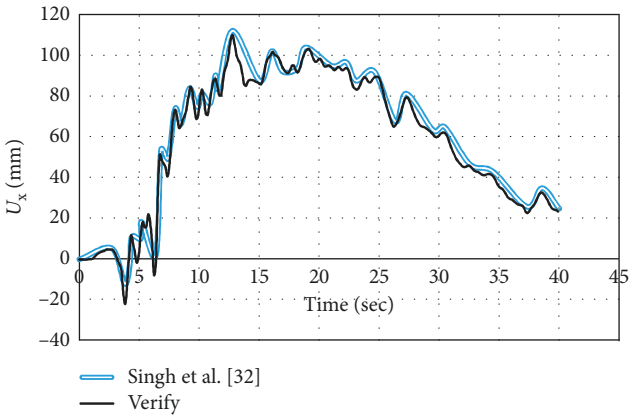

Figure 3: Verification time-history analysis with the result of Singh et al. [32] for horizontal displacement of the tunnel crown.

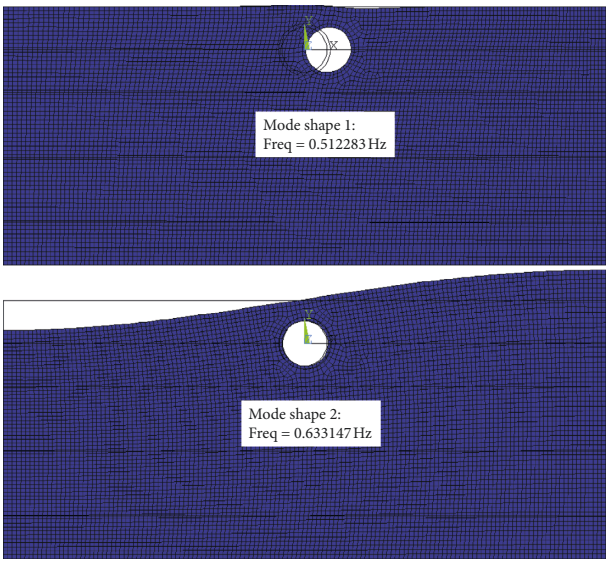

Figure 4: The first and second vibration frequencies and modes for model 4 in Table 2.

Table 5: The first and second mode frequencies and Rayleigh's alpha and beta for all models of Table 2 due to modal analysis.

No.	ω_{n1} (rad/s)	ω_{n2} (rad/s)	α	β
1	3.1393	3.9781	0.1755	0.0141
2	3.1339	3.9781	0.175	0.0141
3	3.2084	3.9783	0.178	0.0139
4	3.21875	3.9782	0.178	0.0139
5	3.1854	3.9823	0.177	0.014
6	3.49	4.4462	0.196	0.0126
7	3.5024	4.44762	0.196	0.0126
8	3.5932	4.4478	0.199	0.0124
9	3.5374	4.4521	0.197	0.0125
10	3.8437	4.8721	0.215	0.0115
11	3.8354	4.87204	0.215	0.0114
12	3.9391	4.8722	0.218	0.01135
13	3.933	4.8723	0.218	0.0114
14	3.8707	3.87682	0.216	0.0114
15	3.895	4.8771	0.217	0.0114
16	4.1274	5.2608	0.231	0.0107
17	4.1416	5.2624	0.232	0.0106
18	4.2452	5.2627	0.235	0.0105
19	4.1767	5.26745	0.233	0.0106
20	4.4372	5.6258	0.248	$9.937 * 10^{-3}$
21	4.4265	5.6257	0.248	$9.948 * 10^{-3}$
22	4.5452	5.626	0.251	$9.832 * 10^{-3}$
23	4.5355	5.626	0.251	$9.841 * 10^{-3}$
24	4.4614	5.6311	0.249	$9.908 * 10^{-3}$
25	4.4915	5.6314	0.25	$9.879 * 10^{-3}$
26	4.6785	5.9652	0.262	$9.3953 * 10^{-3}$
27	4.6941	5.967	0.263	$9.38 * 10^{-3}$
28	4.808	5.9673	0.266	$9.281 * 10^{-3}$
29	4.7286	5.9725	0.264	$9.345 * 10^{-3}$
30	4.95982	6.2901	0.277	$8.889 * 10^{-3}$
31	4.9471	6.2895	0.277	$8.899 * 10^{-3}$
32	4.9814	6.2958	0.278	$8.868 * 10^{-3}$
33	5.0654	6.2901	0.281	$8.806 * 10^{-3}$
34	4.9309	6.2876	0.276	$8.914 * 10^{-3}$
35	3.1683	3.9822	0.176	0.014
36	3.1227	3.9768	0.175	0.014

the center of the tunnel projection onto the ground surface was investigated. With an increase of 14.5% in the friction angle, the maximum acceleration from the center of the tunnel projection onto the ground surface increases by about 12.5%.

The effect of increasing cohesion (C) from zero to 5 was also investigated. With an increase of 5 units in soil cohesion, the maximum acceleration of the ground's surface increases by 13%. The effect of increasing soil cohesion on the maximum acceleration of the ground's surface from zero to 10 was also investigated, and it was determined that this increase would increase the maximum acceleration of the ground's surface by 15.5%. Due to the fact that Poisson's ratio (υ) can be effective in accelerating the maximum ground surface, therefore, the effect of Poisson's ratio of soil on the maximum acceleration from the center of the tunnel projection onto the ground surface was investigated. By decreasing Poisson's ratio from 0.25 to 0.2, in other words, with a 25% decrease in Poisson's ratio of soil, the maximum acceleration of the ground's surface at the mentioned point is reduced by 5.85%. In addition, Poisson's ratio of soil increased from 0.25 to 0.3 to the original model of the Delhi subway. With a 20% increase in Poisson's ratio of soil, the acceleration of the maximum surface area increased by 5.89%. By examining the above, it is determined that the friction angle of the soil is the most important factor among all soil parameters in changing the maximum acceleration of the ground's surface.

4.2. Generating the Acceleration Spectrum. The acceleration spectrum was obtained for the presence of a tunnel (SF) for the points in the distance of zero, 5.83, 10.50, 15.17, 26.83, 38.5, or 51.33 m from the center of the tunnel as projected onto the ground and was compared with the spectrum due to the absence of a tunnel, i.e., the free field (we call it FF). The results are presented in Figures 5–11. These graphs are plotted on the vertical axis for mean values (μ) and mean plus standard deviation ($\mu + \sigma$) of the spectral acceleration log and the main period of the soil-tunnel system in Table 2 with units per second in the horizontal axis.

By comparing the spectral acceleration graphs without the presence of a tunnel and with the presence of a tunnel, it is observed that the presence of the tunnel causes oscillation and irregularities in the spectral acceleration. This is due to the interference of the waves into the tunnel and their refraction and reflection. At peaks, amplification of spectral acceleration due to the convergence of waves and in the valleys, there is an attenuation of spectral acceleration due to the divergence of waves. While the spectral acceleration diagram without a tunnel is smooth, it changes without severe oscillation due to the absence of a tunnel and the propagation of waves without dealing with obstacles such as tunnels. Figure 5 shows the comparison of the acceleration spectrum with the presence and absence of a tunnel for the tunnel center image on the ground surface. It is noticeable that the effect of the tunnel in most of the considered period is to reduce spectral acceleration compared to models without the presence of tunnels. But in some areas of the long period, the tunnel amplifies spectral acceleration than free-field models. Amplification of ground acceleration is observed at three points. The characteristics of these points are presented in Table 6.

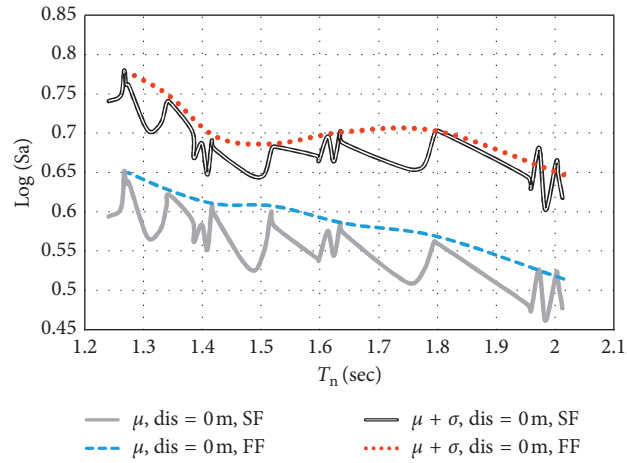

Figure 5: Mean and $\mu + \sigma$ for log of the spectral acceleration of models in the presence (SF) and absence (FF) of a tunnel as determined from the center of the tunnel projection onto the ground surface.

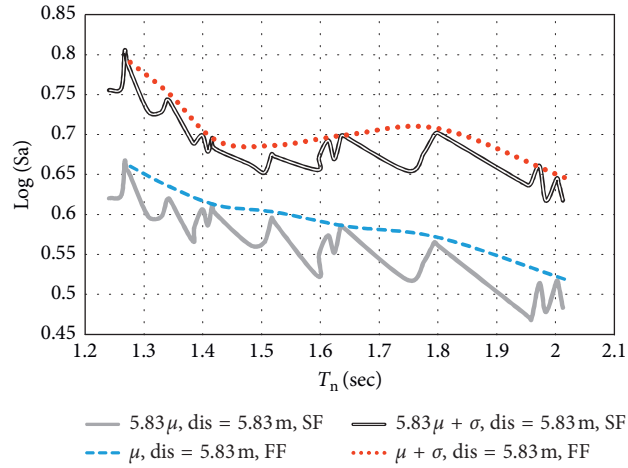

Figure 6: Mean and $\mu + \sigma$ for log of the spectral acceleration for models in the presence (SF) and absence (FF) of a tunnel at a distance of 5.83 m from the center of the tunnel projection onto the ground surface.

The maximum acceleration spectrum from the center of the tunnel projection onto the ground surface for $\mu + \sigma$ and the mean of the data are, respectively, 5.902 and 4.657 m/s^2. They occur at a period of 1.267 seconds. The maximum amount of attenuation for spectral acceleration occurs in the image of the tunnel center on the ground surface. Its value is 15.3%, and it occurred in periods of 1.48 sec, which correspond to a tunnel model with a radius of 6, a thickness of 0.5, and a depth of 10 m and in soil with a modulus of elasticity of 1.75 times greater than that for the Delhi subway.

Figure 6 presents the ground surface acceleration at a point 5.83 m from the center of the tunnel projection onto the ground surface. Three points were observed where the acceleration has amplified owing to the presence of a tunnel.

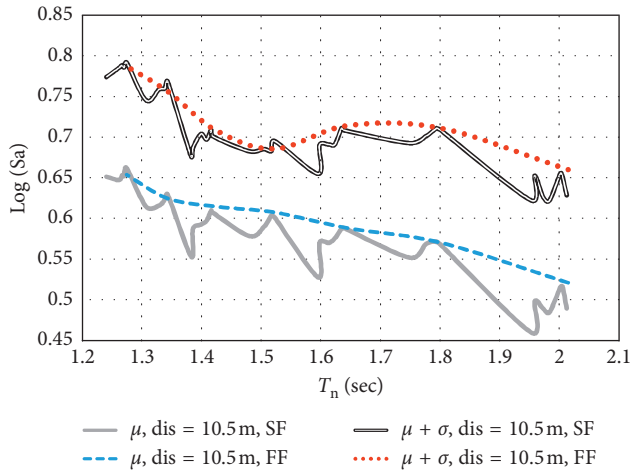

Figure 7: Mean and $\mu + \sigma$ for log of the spectral acceleration for models in the presence (SF) and absence (FF) of a tunnel at a distance of 10.5 m from the center of the tunnel projection onto the ground surface.

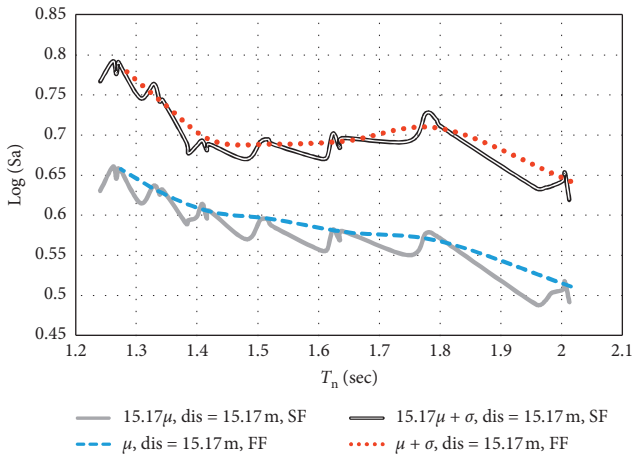

Figure 8: Mean and $\mu + \sigma$ for log of the spectral acceleration for models in the presence (SF) and absence (FF) of a tunnel at a distance of 15.17 m from the center of the tunnel projection onto the ground surface.

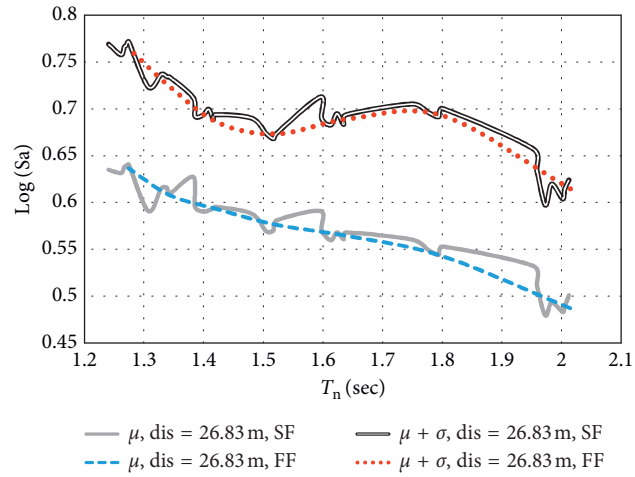

Figure 9: Mean and $\mu + \sigma$ for log of the spectral acceleration for models in the presence (SF) and absence (FF) of a tunnel at a distance of 26.83 m from the center of the tunnel projection onto the ground surface.

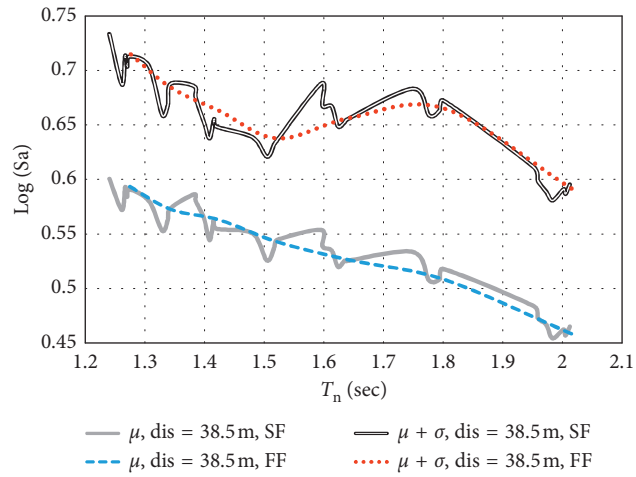

Figure 10: Mean and $\mu + \sigma$ for log of the spectral acceleration for models in the presence (SF) and absence (FF) of a tunnel at a distance of 38.5 m from the center of the tunnel projection onto the ground surface.

The properties of these points are presented in Table 7. The maximum acceleration spectrum in the presence of a tunnel (SF) for $\mu + \sigma$ and the average data was 6.24 and 4.852 m/s^2, respectively, at 5.83 m from the center of the tunnel projection onto the ground surface. It occurred in 1.267 sec periods.

In Figure 7, which provides acceleration spectrum of the ground's surface at a distance of 10.5 m from the center of the tunnel projection onto the ground surface, three points were seen where acceleration amplification occurred due to the presence of the tunnel. The characteristics of these points are presented in Table 8. The maximum value of the acceleration spectrum in the presence of a tunnel for a distance of 10.5 m from the center of the tunnel projection onto the ground surface for $\mu + \sigma$ and the mean of the data was 6.094 and 4.78 m/s^2, respectively. They occur at a period of 1.274 seconds.

As the distance from the center of the tunnel projection onto the ground surface and the spectral acceleration values due to the presence of the tunnel and the absence of the tunnel are closer to each other; so, at a distance of 15.17 meters from the center of the tunnel projection, the presence of the tunnel has increased the spectral acceleration of the models with respect to without the presence of tunnels in more points and cannot ignore the effect of the presence of the tunnel. There are ten points (for the SF model), which amplified acceleration at 15.17 m from the center of the tunnel projection, as a result of the presence of the tunnel, as shown in Figure 8. The characteristics of these points are presented in Table 9. The maximum value of the acceleration spectrum in the presence of a tunnel (SF) at 15.17 m from the center of the tunnel projection onto the ground surface, for the $\mu + \sigma$ and the average data, was 6.04 and 4.76 m/s^2, respectively. They occurred in periods of 1.27 and 1.261 sec.

Figure 9 shows the ground surface acceleration at a point 26.83 m from the center of the tunnel projection onto the

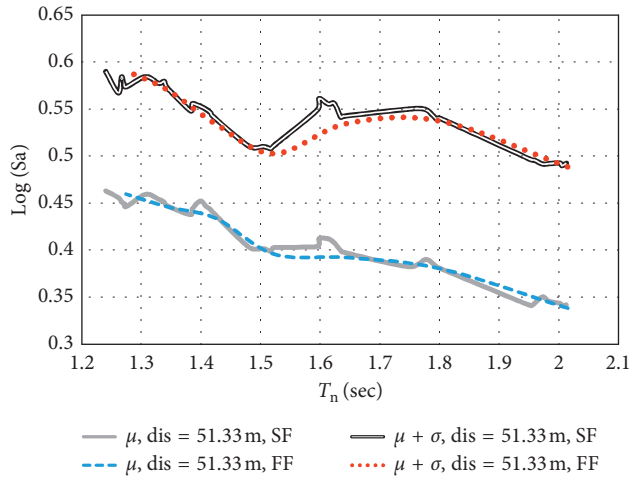

Figure 11: Mean and $\mu + \sigma$ for log of the spectral acceleration for models in the presence (SF) and absence (FF) of a tunnel at a distance of 51.33 m from the center of the tunnel projection onto the ground surface.

Table 6: Properties of models that presence of the tunnel amplifies the acceleration spectrum in the tunnel center image on the ground surface.

No.	Elasticity module of soil (compared to Delhi Metro)	Overburden depth (m)	Lining thickness (m)	Tunnel radius (m)	T_n (sec)
1	1	20	0.75	6	1.973
2	1.5	20	0.5	3.13	1.635
3	1	20	0.5	3.13	2.0015

Table 7: Properties of models that presence of the tunnel amplifies the acceleration spectrum at a distance of 5.83 m from the center of the tunnel projection onto the ground surface.

No.	Elasticity module of soil (compared to Delhi Metro)	Overburden depth (m)	Lining thickness (m)	Tunnel radius (m)	T_n (sec)
1	1	20	0.75	6	1.973
2	2	20	0.5	3.13	1.416
3	2.5	20	0.5	3.13	1.267

Table 8: Properties of models that presence of the tunnel amplifies the acceleration spectrum at a distance of 10.5 m from the center of the tunnel projection onto the ground surface.

No.	Elasticity module of soil (compared to Delhi Metro)	Overburden depth (m)	Lining thickness (m)	Tunnel radius (m)	T_n (sec)
1	2.25	20	0.28	3.13	1.339
2	2.25	10	0.28	3.13	1.343
3	2.5	10	0.28	3.13	1.2743

Table 9: Properties of models that presence of the tunnel amplifies the acceleration spectrum at a distance of 15.17 m from the center of the tunnel projection onto the ground surface.

No.	Elasticity module of soil (compared to Delhi Metro)	Overburden depth (m)	Lining thickness (m)	Tunnel radius (m)	T_n (sec)
1	1	20	0.28	3.13	2.005
2	1.25	20	0.28	3.13	1.794
3	1.5	20	0.28	3.13	1.6382
4	1.75	20	0.28	3.13	1.5171
5	2.5	20	0.28	3.13	1.27
6	1.25	20	0.5	6	1.7762
7	1.5	20	0.5	6	1.6233
8	2.25	20	0.5	6	1.3287
9	2.5	20	0.5	6	1.2613
10	1.25	10	0.28	3.13	1.8003

ground surface. Twenty-four points were observed where the acceleration has amplified due to the presence of a tunnel. The characteristics of these points are presented in Table 8. The maximum amount of amplification of spectral acceleration occurs at a distance of 26.83 m from the center of the tunnel projection onto the ground surface. Its value is 11.47%, and occurred in period of 1.952 sec, which corresponds to a model with a tunnel radius of 6 m, thickness of 0.75 m, anddepth of 10 meters and on a soil with an elastic modulus equal to the Delhi subway. The maximum value of the acceleration spectrum in the presence of a tunnel for a distance of 26.83 meters from the center of the tunnel projection onto the ground surface for the $\mu + \sigma$ and the mean of the data was, respectively, 5.759 and 4.547 m/s^2. They occur at a period of 1.274 seconds.

Figure 10 presents the ground surface acceleration at a point 38.5 m from the center of the tunnel projection onto the ground surface. Fourteen points were observed where the acceleration has amplified due to the presence of a tunnel. The maximum value of acceleration spectrum in the presence of a tunnel for a distance of 38.5 m from the center of the tunnel projection onto the ground surface for the $\mu + \sigma$ and the average data was 5.233 and 4.147 m/s^2, respectively. They occur at 1.24 sec periods.

Figure 11 provides the ground surface acceleration at a distance of 51.33 m from the center of the tunnel projection onto the ground surface. Twenty-eight points are observed where the acceleration amplification occurred due to the presence of a tunnel. The maximum value of the acceleration spectrum in the presence of a tunnel for a distance of 51.33 m from the center of the tunnel projection onto the ground surface for the $\mu + \sigma$ and the average data was 3.818 and 3.014 m/s^2, respectively. They occur at a period of 1.307 and 1.24 sec.

As taking the distance from the center of the tunnel projection onto the ground surface, the number of points in which the acceleration amplification of the ground occurred due to the presence of the tunnel in them, increases. But after 26.83 meters, its difference is negligible. So that the maximum acceleration amplification value of the SF model relative to FF is at 51.33 m from the tunnel center image of 6.4%.

As we can see, the use of ground surface acceleration spectra without the effect of the tunnel presence does not seem to be a reliable method. Thus, the effect of the presence of the tunnel, particularly at farther distances from the center of the tunnel projection onto the ground surface, is inevitable in computing the spectral acceleration. The curves are obtained by assuming the soil and structure interaction as well as the assumption of a flexible foundation for the ground surface structure. Therefore, for the period of the ground surface structures, an equivalent period which involves the effects of substructure soil can be used. In NIST,[40] several relations have been suggested for the equivalent period of structure and soil below it. The maximum value of the acceleration spectrum in the presence of the tunnel for the different points of the tunnel center image is summarized in Table 10.

The absolute maximum of the acceleration spectrum in the presence of a tunnel (SF) between all curves is at 5.83 m from the center of the tunnel projection onto the ground surface. This value is 6.24 and 4.852 m/s^2 for $\mu + \sigma$ and the mean data, respectively, and occurs at period of 1.267 sec, which corresponds to a model with a tunnel radius of 3.13 m, a tunnel lining thickness 0.5 m, and a tunnel depth of 20 m in soil with a modulus of elasticity that is 2.5 times that of the Delhi subway.

Figure 12 displays and compares the average spectral accelerations for models in the presence of a tunnel (SF) at distances of zero, 5.83, 10.50, 15.17, 26.83, 38.5, and 51.33 m from the center of the tunnel projection onto the ground surface. As these graphs show, the value of spectral acceleration at a 26.83 m distance from the center of the tunnel projection onto the ground surface was greater than the other points for a large range of the period under review. This process, however, is reversible for the 51.33 m distance from the image of the tunnel center on the ground surface.

The ratio of SF/FF (for the average of spectral accelerations) versus the increase in distance from the image of the tunnel center onto the ground surface is shown in Figure 13. These graphs were drawn for the points zero, 5.83, 10.50, 15.17, 26.83, 38.5, and 51.33 m from the center of the tunnel projection onto the ground surface.

The models 10–14 of Table 2 were used in Figure 13. In these models, the soil in which the tunnel is excavated is similar and its elastic modulus is 1.5 times the Delhi subway soil. It can be seen that in all models, the models are closed to

Table 10: Maximum acceleration spectrum for SF models at different distances from the center of the tunnel image on the ground surface.

Distance (m)	Zero	5.83	10.5	15.17	26.83	38.5	51.33
$Sa_{(\mu)}$ (m/s^2)	4.657	4.852	4.78	4.76	4.547	4.147	3.014
$Sa_{(\mu+\sigma)}$ (m/s^2)	5.902	6.24	6.094	6.04	5.759	5.233	3.818

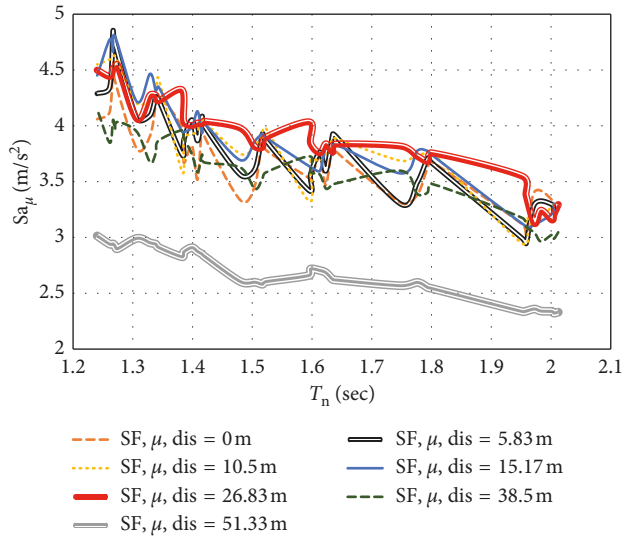

Figure 12: Average spectral accelerations for models with the presence of a tunnel (SF) at distances of zero, 5.83, 10.50, 15.17, 26.83, 38.5, and 51.33 meters from the center of the tunnel projection onto the ground surface and their comparison.

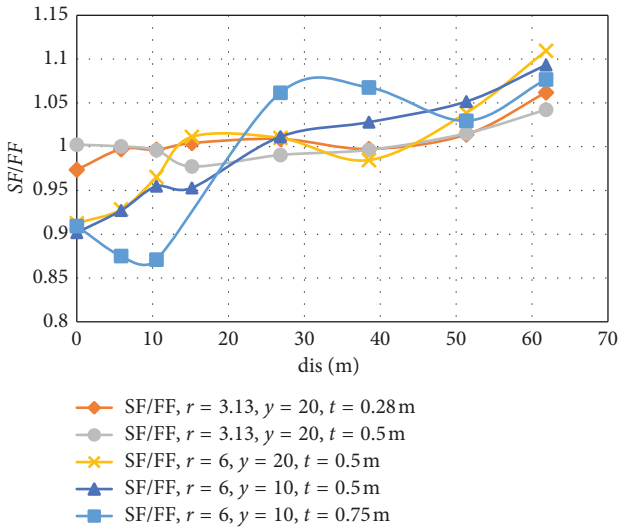

Figure 13: The ratio of SF/FF (for average of spectral accelerations) for models 10–14 of Table 2 at distances of zero, 5.83, 10.50, 15.17, 26.83, 38.5, 51.33, and 61.83 meters from the center of the tunnel projection onto the ground surface and their comparison.

each others after 38.5 meters. This process is independent of the radius, lining thickness, and the depth of the tunnel placement. But the effect of the presence of the tunnel is still observed, and the SF/FF ratio is larger than one.

5. Conclusions

This study indicates that the acceleration of the ground surface depends on the presence of the tunnel at the distance of the point under consideration from the image of tunnel center. Just above the image of the tunnel center on the ground surface, the presence of the tunnel can be effective at a small point in the range of a long period of amplification of the spectral acceleration, but in a wide range of long periods, it causes to decrease the spectral acceleration. With increasing distance from the center of the tunnel projection onto the ground surface, in long periods, amplification of spectral acceleration is observed due to the presence of a tunnel. In the distance of 51.33 meters from the tunnel center, the highest number of acceleration amplification is observed on the ground. In other words, the position of the points on the surface of the ground toward the tunnel effected amplification or attenuation of the acceleration on the ground surface.

(i) Spectral acceleration of the ground surface due to the presence of the tunnel, except for a few exceptions, at a distance of 26.86 meters from the image of the center of the tunnel on the ground surface is larger than the rest of the studied points (zero, 5.83, 10.50, 15.17, 26.83, 38.5, and 51.33 m) in most of the studied range.

(ii) For the models studied, the spectral accelerations of the ground surface converged to each other after 38.5 meters. This trend is independent of tunnel radius, the thickness of the coating, and the depth of the tunnel placement.

(iii) Acceleration amplification due to the presence of the tunnel strongly depends on the model used. In the distances of zero–15.17 m from the center of the tunnel projection onto the ground surface, amplification of the ground surface acceleration was primarily observed in most cases (16 out of 19 cases) at the 20 m depth. This is why such an overburden depth amplifies the acceleration at the ground surface. As the overburden depth increases, the waves interfere with the tunnel sooner and were disrupted because the waves propagated from the bottom of the model. At a distance of zero to 15.17 m from the image of the tunnel center onto the ground surface, 13 out of 19 ground amplification accelerates are related to a tunnel with a lower radius (3.13 meters). Therefore, the tunnel properties contributed to the amplification of ground surface acceleration. For points with a distance of 26.83, 38.5, and 51.33 meters, the image of the tunnel center on the ground surface has been shown to amplify spectral acceleration due to the presence of a tunnel for most models.

(iv) According to the present study, it is recommended that the horizontal component of the accelerated spectral modification of the ground surface be used to design new structures within a distance of zero to 50 meters from the tunnel center image of the ground. The presence of the tunnel causes an increase in the ground surface above 11% and a decrease above 15%.

(v) This study showed that amplification in the acceleration spectrum due to the presence of a tunnel is highly dependent on the characteristics of the model under study. Therefore, it is suggested that SSI analysis be performed by the presence of a tunnel. In the absence of accurate analysis, it is suggested that for confidence, the spectral acceleration be increased to 15%.

Data Availability

The data used to support the findings of this study are available from the corresponding author upon request.

Conflicts of Interest

The authors declare that they have no conflicts of interest.

References

[1] U. Cilingir and S. P. G. Madabhushi, "A model study on the effects of input motion on the seismic behaviour of tunnels," *Soil Dynamics and Earthquake Engineering*, vol. 31, no. 3, pp. 452–462, 2011.

[2] G. D. Hatzigeorgiou and D. E. Beskos, "Soil-structure interaction effects on seismic inelastic analysis of 3-D tunnels," *Soil Dynamics and Earthquake Engineering*, vol. 30, no. 9, pp. 851–861, 2010.

[3] J. Luzhen, C. Jun, and L. Jie, "Seismic response of underground utility tunnels: shaking table testing and FEM

analysis," *Earthquake Engineering and Engineering Vibration*, vol. 9, no. 4, pp. 555–567, 2010.

[4] Y. B. Yang and L. C. Hsu, "A review of researches on ground-borne vibrations due to moving trains via underground tunnels," *Advances in Structural Engineering*, vol. 9, no. 3, pp. 377–392, 2006.

[5] P. Yiouta-Mitra, G. Kouretzis, G. Bouckovalas, and A. Sofianos, "Effect of underground structures in earthquake resistant design of surface STRUCTURES," in *Proceedings of the ASCE GSP 160 Dynamic Response and Soil Properties, Geo-Denver, New Peaks in Geotechnics*, Denver, CO, USA, October 2007.

[6] M. H. Baziar, M. R. Moghadam, K. Dong-Soo, and C. Y. Wook, "Effect of underground tunnel on the ground surface acceleration," *Tunnelling and Underground Space Technology*, vol. 44, pp. 10–22, 2014.

[7] V. Besharat, M. Davoodi, and M. K. Jafari, "Effect of underground structures on free-field ground motion during earthquakes," in *Proceedings of The Fifthteenth World Conference on Earthquake Engineering*, Lisboa, Portugal, 2012.

[8] V. Besharat, M. Davoodi, and M. K. Jafari, "Variations in ground surface responses under different seismic input motions due the presence of a tunnel," *Arabian Journal for Science and Engineering*, vol. 39, no. 10, pp. 6927–6941, 2014.

[9] Y.-h. Pao and C. C. Mow, *The Diffraction of Elastic Waves and Dynamic Stress Concentrations*, Crane-Russak, New York, NY, USA, 1973.

[10] M. Dravinski, "Ground motion amplification due to elastic inclusions in a halfspace," *Earthquake Engineering and Structural Dynamics*, vol. 11, no. 3, pp. 313–335, 1983.

[11] K. C. Wong, A. H. Shah, and S. K. Datta, "Diffraction of elastic waves in a halfspace. II. Analytical and numerical solutions," *Bulletin of the Seismological Society of America*, vol. 75, no. 1, pp. 69–92, 1985.

[12] V. W. Lee, "Three dimensional diffraction of elastic waves by a spherical cavity in an elastic halfspace: closed form solutions," *Soil Dynamics and Earthquake Engineering*, vol. 7, no. 3, pp. 149–161, 1988.

[13] C. Smerzini, J. Avilés, R. Paolucci, and F. J. Sánchez-Sesma, "Effect of underground cavities on surface ground motion under SH wave propagation," *Earthquake Engineering & Structural Dynamics*, vol. 38, no. 12, pp. 1441–1460, 2009.

[14] J. Li, Q. Yue, and J. Chen, "Dynamic response of utility tunnel during the passage of Rayleigh waves," *Earthquake Science*, vol. 23, pp. 13–24, 2010.

[15] C. Sun and Q. Wang, "Effects of underground structure on acceleration response of site," *Advanced Materials Research*, vol. 368–373, pp. 2791–2794, 2012.

[16] V. Raghavendra, S. Jose, G. H. A. Shounak, and T. G. Sitharam, "Finite element analysis of underground metro tunnels," *International Journal of Civil Engineering and Technology (IJCIET)*, vol. 6, no. 2, pp. 6–15, 2015.

[17] A. M. Marshall and T. Haji, "An analytical study of tunnel–pile interaction," *Tunnelling and Underground Space Technology*, vol. 45, pp. 43–51, 2015.

[18] B. Sevim, "Assessment of 3D earthquake response of the Arhavi Highway Tunnel considering soil-structure interaction," *Computers and Concrete*, vol. 11, no. 1, pp. 51–61, 2013.

[19] G. Zheng, J. Sun, T. Zhang, Q. Fan, and H. Zhou, "Eulerian finite element model for stability analysis of circular tunnels in undrained clay," *Engineering Failure Analysis*, vol. 91, pp. 216–224, 2018.

[20] S. Rezaeian and A. Der Kiureghian, *Stochastic Modeling and Simulation of Ground Motions for Performance-Based Earthquake Engineering*, Pacific Earthquake Engineering, Berkeley, CA, USA, 2010.

[21] International Code Council, *International Building Code*, International Code Council, Washington, DC, USA, 2006.

[22] Building Seismic Safety Council for the Federal Emergency Management Agency, *NEHRP Recommended Provisions for New Buildings and Other Structures, FEMA-450*, Building Seismic Safety Council for the Federal Emergency Management Agency, Washington, DC, USA, 2003.

[23] N. A. Abrahamson and W. J. Silva, "Summary of the abrahamson & silva NGA ground-motion relations," *Earthquake Spectra*.vol. 24, no. 1, pp. 67–97, 2008.

[24] D. M. Boore and G. M. Atkinson, "Ground-motion prediction equations for the average horizontal component of PGA, PGV, and 5%-damped PSA at spectral periods between 0.01 s and 10.0 s," *Earthquake Spectra*, vol. 24, no. 1, pp. 99–138, 2008.

[25] K. W. Campbell and Y. Bozorgnia, "NGA ground motion model for the geometric mean horizontal component of PGA, PGV, PGD and 5% damped linear elastic response spectra for periods ranging from 0.01 to 10 s," *Earthquake Spectra*, vol. 24, pp. 139–171, 2008.

[26] B.-J. Chiou and R. R. Youngs, "An NGA model for the average horizontal component of peak ground motion and response spectra," *Earthquake Spectra*, vol. 24, no. 1, pp. 173–215, 2008.

[27] I. M. Idriss, "An NGA empirical model for estimating the horizontal spectral values generated by shallow crustal earthquakes," *Earthquake Spectra*, vol. 24, no. 1, pp. 217–242, 2008.

[28] Plaxis 2D Version 8.5. Finite Element Code for Geotechnical Engineering, http://www.plaxis.nl/.

[29] ANSYS Multiphysics Simulation Software version 15. Finite Element Code for Mechanical Engineering, http://www.ansys.com/.

[30] M. Monjezi, B. N. Rahmani, S. R. Torabi, and T. N. Singh, "Stability analysis of a shallow depth metro tunnel: a numerical approach/Analiza stabilności płytkiego tunelu metra z wykorzystaniem metod numerycznych," *Archives of Mining Sciences*, vol. 57, no. 3, pp. 535–545, 2012.

[31] U. Cilingir and S. P. G. Madabhushi, "Effect of depth on seismic response of circular tunnels," *Canadian Geotechnical Journal*, vol. 48, no. 1, pp. 117–127, 2011.

[32] M. Singh, M. N. Viladkar, and N. K. Samadhiya, "Seismic analysis of Delhi metro underground tunnels," *Indian Geotechnical Journal*, vol. 47, no. 1, pp. 67–83, 2016.

[33] Pacific Earthquake Engineering Research Center (PEER), *PEER Ground Motion Database*, Pacific Earthquake Engineering Research Center (PEER), Berkeley, CA, USA, 2017.

[34] Regulations of design Building against Earthquake, Standard 2800, in Persian.

[35] J. Lysmer and R. L. Kuhlemeyer, "Finite dynamic model for infinite media," *Journal of Engineering Mechanics Division*, vol. 95, pp. 859–878, 1969.

[36] R. L. Kuhlemeyer and J. Lysmer, "Finite element method accuracy for wave propagation problems," *Journal of the Soil Dynamics Division*, vol. 99, pp. 421–427, 1973.

[37] B. Sevim, "Nonlinear earthquake behaviour of highway tunnels," *Natural Hazards and Earth System Sciences*, vol. 11, no. 10, pp. 2755–2763, 2011.

[38] R. I. Dobry, I. Oweis, and A. Urzua, "Simplified procedures for estimating the fundamental period of a soil profile," *Bulletin of the Seismological Society of America*, vol. 66, no. 4, pp. 1293–1321, 1976.

[39] A. Rastbood, Y. Gholipour, and A. Majdi, "Stress analysis of segmental tunnel lining using artificial neural network," *Periodica Polytechnica Civil Engineering*, vol. 61, no. 4, pp. 664–676, 2017.

[40] National Institute of Standards and Technology, *Soil-Structure Interaction for Building Structures*, National Institute of Standards and Technology, Gaithersburg, MD, USA, 2012.